

Static Light Scattering From Concentrated Protein Solutions II: Experimental Test of Theory for Protein Mixtures and Weakly Self-Associating Proteins

Cristina Fernández and Allen P. Minton*

Laboratory of Biochemistry and Genetics, National Institute of Diabetes and Digestive and Kidney Diseases, National Institutes of Health, U.S. Department of Health and Human Services, Bethesda Maryland

ABSTRACT Using an experimental technique recently developed in this laboratory (Fernández C. and A. P. Minton. 2008. *Anal. Biochem.* 381:254–257), the Rayleigh light scattering of solutions of bovine serum albumin, hen egg white ovalbumin, hen egg white ovomucoid, and binary mixtures of these three proteins was measured as a function of concentration at concentrations up to 125 g/L. The measured concentration dependence of scattering of both pure proteins and binary mixtures is accounted for nearly quantitatively by an effective hard particle model (Minton A. P. 2007. *Biophys. J.* 93:1321–1328) in which each protein species is represented by an equivalent hard sphere, the size of which is determined by the nature of repulsive interactions between like molecules under a given set of experimental conditions. The light scattering of solutions of chymotrypsin A was measured as a function of concentration at concentrations up to 70 g/L at pH 4.1, 5.4, and 7.2. At each pH, the measured concentration dependence is accounted for quantitatively by an effective hard particle model, according to which monomeric protein may self-associate to form an equilibrium dimer and, depending upon pH, an equilibrium pentamer or hexamer.

INTRODUCTION

Interest in the physical properties of highly concentrated protein solutions has increased significantly in recent years, as it has become more widely recognized that an understanding of those properties is prerequisite to an understanding of chemical equilibria and rate processes in biological fluids (1,2) and in biopharmaceutical formulations (3). Weakly attractive and repulsive interactions between protein molecules that are undetectable at the low protein concentrations ordinarily encountered in a biophysical experiment (typically <5 g/L) exert an ever-greater influence upon solution properties as protein concentrations approach the saturation limit, which, depending upon experimental conditions, may be as large as several hundred g/L. With few exceptions, one cannot reliably predict the behavior of a protein at a high concentration on the basis of knowledge obtained from experiments carried out at low concentrations. Quantitative characterization of the concentration-dependent behavior of protein solutions in the high concentration regime (>50 g/L), therefore, presents both experimental and theoretical challenges to the investigator.

We have recently presented an approximate theory for the interpretation of the light scattering of multiple species of proteins at arbitrary concentrations (5), in which each species is treated as an effective hard convex particle, the size of which reflects not only steric repulsion but also short-ranged “soft” electrostatic repulsion between macromolecules. Attractive intermolecular interactions are treated as equilib-

rium associations. The effective hard particle model has been shown to account quantitatively for the concentration dependence of thermodynamically-based solution properties (e.g. sedimentation equilibrium, osmotic pressure, and static light scattering) of individual proteins over a broad range of concentrations (6–11).

Concurrently, we have also developed an efficient experimental method for measuring the concentration dependence of the static light scattering of protein solutions over a broad range of concentrations (12). In this study, we employed the newly developed experimental methodology to measure the concentration dependence of light scattering of three globular proteins (bovine serum albumin, hen egg ovalbumin, and hen egg ovomucoid) and mixtures of these proteins, and compared the observed results with predictions of the approximate theory. We additionally measured the concentration and pH dependence of light scattering of a protein, chymotrypsin A, that is known to self-associate with an affinity that changes with pH (13–15), and interpreted the results in the context of models for self-association and nonspecific repulsive interaction.

MATERIALS AND METHODS

Materials

Monomeric bovine serum albumin (BSA) was obtained from Sigma-Aldrich (St. Louis, MO) (A1900). Albumin (chicken egg white), ovomucoid (Trypsin inhibitor) and inactivated chymotrypsin A were obtained from Worthington Biochemical Corporation (Lakewood, NJ) (LS003048, LS003087, and LS001434, respectively). All proteins elute from a size exclusion chromatography column with an on line light scattering detector as a single peak corresponding to the monomer, except for BSA, which shows a small additional

Submitted August 28, 2008, and accepted for publication November 25, 2008.

*Correspondence: minton@helix.nih.gov

Editor: Kathleen B. Hall.

© 2009 by the biophysical society
0006-3495/09/03/1992/7 \$2.00

doi: 10.1016/j.bpj.2008.11.054

peak (<3% of total protein) corresponding to the covalent dimer. Before use, BSA, ovalbumin and ovomucoid were dialyzed against phosphate buffer, 0.05 M phosphate, 0.15 M NaCl at pH 7.2. Chymotrypsin A was dialyzed against phosphate buffer, 0.05 M phosphate, 0.20 M NaCl at pH 5.4 and pH 7.2, and citric acid 0.05 M, 0.20 M NaCl at pH 4.1. Dialysis for buffer exchange was performed against excess solvent overnight using Pierce 10000 MWCO Slide-A-Lyzer Dialysis cassettes. To prepare concentrated protein solutions, proteins were dissolved at low concentrations (<30 g/L), dialyzed, and then concentrated using Centricon filter devices (Ultracel YM-10 membrane – 10,000 NMWL; Millipore, Billerica, MA) to different final concentrations. Final concentrations were determined from the absorbance at 280 nm using the following standard values for absorbance in optical density units per centimeter pathlength for 1 g/L solution: BSA, 0.65 (16); ovalbumin, 0.75 (16); ovomucoid, 0.41 (17); and chymotrypsin A, 2.04 (13). The buffer and protein were prefiltered through 0.02- μ m Whatman Anotop filters (Whatman, Florham Park, NJ). Immediately before measurements of light scattering were taken, protein solutions were centrifuged at 80000 g for 30 min to remove residual particulates and microscopic bubbles.

Experimental Procedures

Measurements were carried out via automated sequential dilution as described in Fernández and Minton (12). Briefly, a MiniDAWN Tristar light scattering detector (Wyatt Technology, Santa Barbara, CA) was modified by the addition of a Variomag Mini cuvette stirrer (Variomag-USA, Daytona Beach, FL) mounted in the base of the MiniDawn read head, and the light scattering flow cell was replaced by a square cuvette holder. A square fluorescence cuvette containing 2 ml of protein solution and a small magnetic stirring bar was inserted into the cuvette holder. The gradient of protein concentration was created by successive dilutions of the initially concentrated solution using a programmable dual-syringe pump to add buffer and remove solution. Although the light scattering apparatus used lacked means for controlling the temperature of the sample, sample temperature was monitored continuously and found to remain constant to within 2°C over the approximately one hour time course of a dilution experiment. Depending upon the ambient temperature in the laboratory during a particular experiment (which varied with the season), average sample temperatures measured during a dilution experiment varied between 26°C and 31°C. However, replicate experiments conducted at different times showed no significant dependence of the measured scattering intensity upon temperature within this limited range of temperatures.

As previously described (18), the baseline-subtracted intensity of light scattered at 90° was converted to the Rayleigh ratio expressed in units of the optical constant K , defined by

$$K = \frac{4\pi\tilde{n}^2(d\tilde{n}/dw)^2}{\lambda_0^4 N_A}, \quad (1)$$

where \tilde{n} denotes the refractive index of solution, λ_0 is the wavelength of incident light in vacuum (690 nm), and N_A is Avogadro's number. The refractive increment $d\tilde{n}/dw$ is equal to 0.185 cm³/g for all proteins studied here (19). It follows that the refractive index of a solution containing multiple species of protein may be expressed as

$$\tilde{n} = \tilde{n}_0 + (d\tilde{n}/dw)w_{tot}, \quad (2)$$

where \tilde{n}_0 denotes the refractive index of solvent (phosphate buffered saline, 1.335) and w_{tot} denotes the total weight/volume concentration of protein.

Analysis

According to the fluctuation theory of light scattering, the static light scattering of a solution of multiple solutes is given by (20,21)

$$\frac{R}{K} = \sum_{i,j} M_i M_j \langle \Delta c_i \Delta c_j \rangle, \quad (3)$$

where M_i denotes the molar mass of the i th scattering species and $\langle \Delta c_i \Delta c_j \rangle$ denotes the mean product of the fluctuations of the molar concentrations of the i th and the j th scattering species about their respective equilibrium values, henceforth referred to as the average co-fluctuation of the two species. It has been pointed out that in principle, salt-protein interactions can under certain conditions contribute significantly to the dependence of solution light scattering on protein concentration (22,23). However, in solutions of moderate ionic strength where approximations underlying the effective hard particle model are expected to be realistic (24), we assume that the influence of salt-protein interactions is taken into account implicitly as a factor affecting protein-protein interactions, and thus the size of the effective hard particle best representing a particular protein species. Accordingly, the summation indicated in Eq. 3 is carried out only over protein species. Justification for this simplification is presented below.

Expressions for average self- and hetero-cofluctuations in mixtures of up to three scattering species are presented by Minton (5) as functions of the molar concentrations of each species, c_i , and partial derivatives of the logarithm of the thermodynamic activity coefficient of each species with respect to the concentrations of all species, $\partial \ln \gamma_i / \partial c_j$. The derivatives are evaluated as a function of the concentrations of all protein species using the scaled particle theory of hard convex particle mixtures (25,26) as described in Minton (5).

In the model presented previously (5), attractive interactions are treated as association equilibria. Whereas such treatment may be formally derived from any attractive potential (27), it is most realistic and useful when the range of attractive interactions is short relative to the size of the interacting molecules (24). According to this picture, an oligomeric species is defined or designated on the basis of stoichiometry and propinquity, and does not necessarily possess a well-defined structure. It follows that oligomeric species whose presence is deduced from analysis of data within the context of this model, particularly those characterized by very low equilibrium

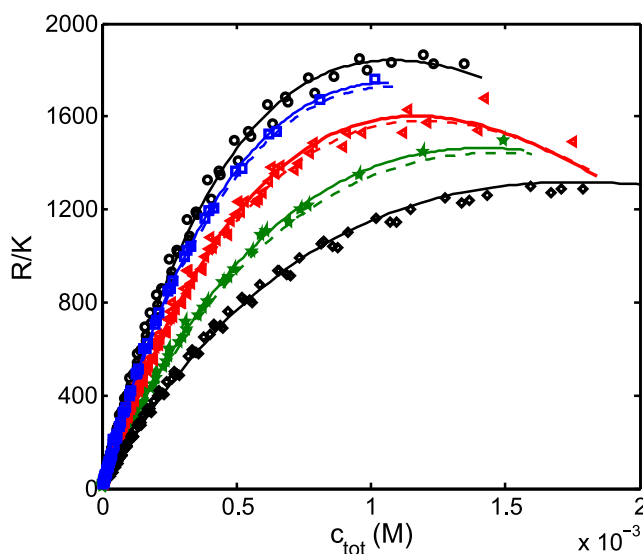


FIGURE 1 Dependence of normalized scattering intensity upon total molar concentration of BSA, ovalbumin, and binary mixtures. Experimental data: circles, squares, triangles, pentagrams and diamonds are results from solutions containing BSA mole fraction 1 (pure BSA), 0.8, 0.5, 0.2, and 0 (pure ovalbumin), respectively. Solid curves for the pure proteins were calculated using the effective hard sphere model for a single species with best-fit parameter values given in Table 1. Dashed curves for the mixtures were calculated using the effective hard sphere model for two species and mole fractions constrained to the values given above. Solid curves for the mixtures were calculated using the effective hard sphere model for two species with adjustable mole fraction of BSA using the following best fit values: 0.84, 0.55, and 0.24 respectively.

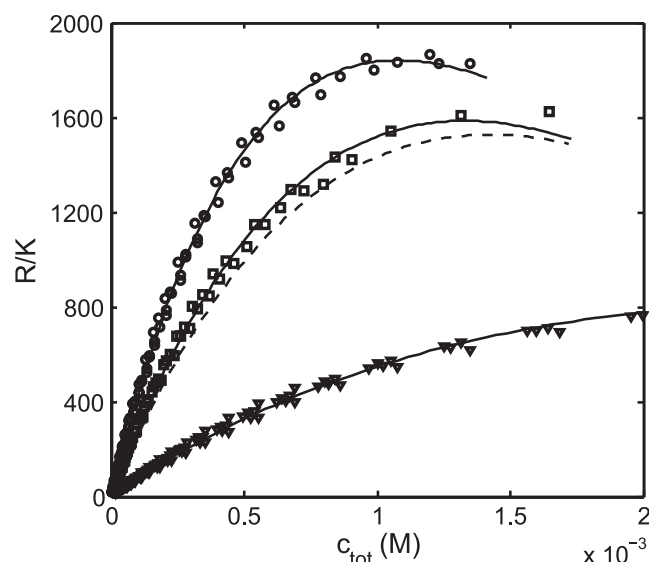


FIGURE 2 Dependence of normalized scattering intensity upon total molar concentration of BSA, ovomucoid, and an equimolar mixture. Experimental data: circles, squares, and triangles, are results from solutions containing BSA mole fraction 1, 0.5, and 0, respectively. Solid curves for the pure proteins were calculated as described above. Dashed curve for the equimolar mixture was calculated using the effective hard sphere model for two species and BSA mole fraction constrained to 0.5. The solid curve for the equimolar mixture was calculated using the effective hard sphere model for two species with adjustable mole fraction of BSA using a best fit value of 0.58.

association constants, may include weakly associated clusters arising from nonspecific attractions in addition to well-structured oligomers resulting from specific interactions (28).

Within the context of the effective hard particle model, the dependence of Rayleigh scattering intensity upon the composition of a solution containing multiple macromolecular scattering species is thus specified by the following parameters: the size or specific volume and shape of the equivalent hard particle representing each scattering species, and, if necessary, one or more association constants governing equilibrium relations between the concentrations of monomeric and oligomeric scattering species as functions of the total specified concentration of each component. The method of numerical calculation of scattering is described in Minton (5).

RESULTS AND DISCUSSION

Nonassociating proteins and protein mixtures

The normalized scattering intensity of pure BSA, ovalbumin, and ovomucoid and binary mixtures of each pair of proteins is plotted as a function of total molar concentration in Figs. 1–3. The results presented for each preparation represent all of the data obtained from two to five replicate experiments, thus providing a measure of experimental precision.

The concentration dependence of scattering intensity of each individual globular protein was presented recently (12) as a validation of the utility of the experimental method used in this study. As reported earlier, all three data sets may be well-described by a non-self-associating equivalent hard sphere model, with best-fit molecular weights and specific volumes presented in Table 1. (The best-fit values of the

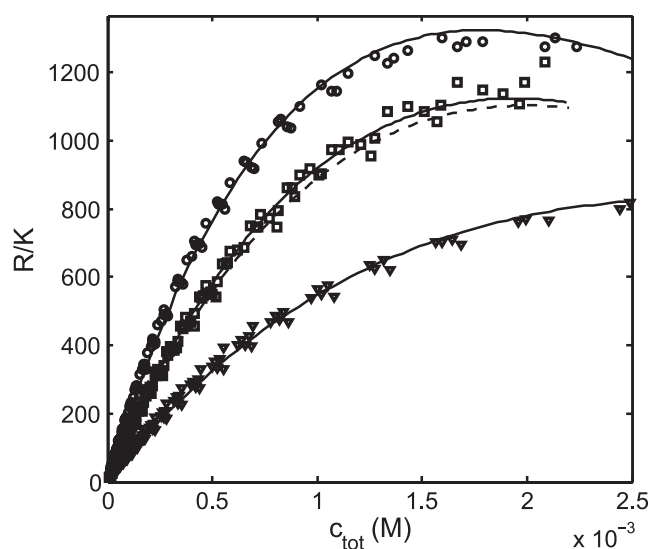


FIGURE 3 Dependence of normalized scattering intensity upon total molar concentration of ovalbumin, ovomucoid, and an equimolar mixture. Experimental data: circles, squares, and triangles are results from solutions containing ovalbumin mole fraction 1, 0.5, and 0, respectively. Solid curves for the pure proteins were calculated as described above. The dashed curve for the equimolar mixture was calculated using the effective hard sphere model for two species and ovalbumin mole fraction constrained to 0.5. The solid curve for the equimolar mixture was calculated using the effective hard sphere model for two species with adjustable mole fraction of ovalbumin using a best fit value of 0.55.

specific volumes of the particles representing each protein vary slightly from those reported earlier due to correction of a minor error in the calculation of normalized scattering intensity).

The effective specific volume of BSA, $1.77 \text{ cm}^3/\text{g}$, is in semiquantitative agreement with values obtained from prior measurements of light scattering, osmotic pressure and sedimentation equilibrium conducted under similar conditions of pH and ionic strength (summarized in (6)).

Given the best-fit values of molar mass and specific volume corresponding to each protein, Eqs. 1–8 and 25–27 of (5) were used to compute the concentration dependence of scattering for binary nonassociating mixtures of the proteins containing specified mole fractions of each species. The results are plotted as dashed curves in Figs. 1–3. Finally, the mole fraction of each species in a mixture was allowed to vary to achieve a best-fit of the model to the experimental data. The best-fit value of mole fraction corresponding to each mixture is presented in the corresponding figure legend. It is evident upon inspection that without any adjustment the

TABLE 1 Best-fit values of effective hard-sphere parameters characterizing globular proteins at high concentration

Protein	MW	$v_{\text{eff}} (\text{cm}^3/\text{g})$
BSA	68700 ± 1600	1.77 ± 0.06
ovalbumin	45500 ± 1000	1.64 ± 0.05
ovomucoid	28000 ± 820	1.61 ± 0.07

Indicated uncertainties correspond to 1 standard error of estimate.

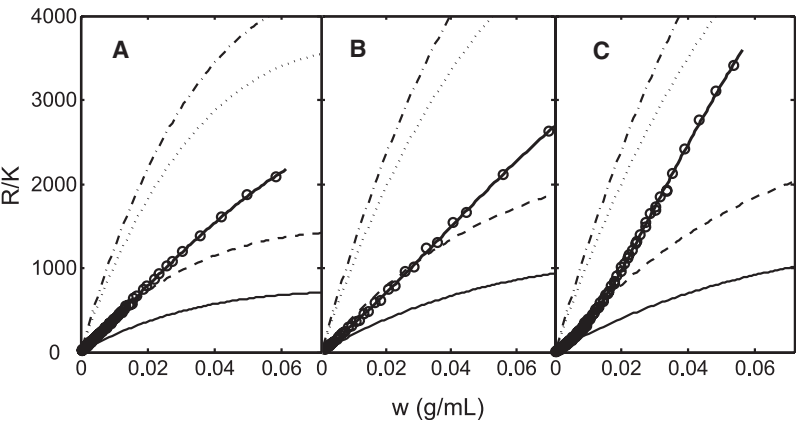


FIGURE 4 Concentration dependence of normalized scattering intensity of chymotrypsin A solutions at pH 4.1 (A), pH 5.4 (B), and pH 7.2 (C). Circles: Experimental data; thick solid curve: best fit of the three species effective hard sphere model with allowance for formation of equilibrium dimer and one higher oligomer, using the best-fit parameter values indicated in Table 2. Best fit curves calculated from the monomer-dimer-pentamer and monomer-dimer-hexamer models at pH 5.4 are indistinguishable. Also plotted in each panel are reference curves calculated according to the one-species effective hard sphere model for hypothetical nonassociating monomer (*thin solid line*), dimer (*dashed*), pentamer (*dotted*) and hexamer (*dot-dashed*).

effective hard particle model provides a nearly quantitative description of the concentration-dependent scattering of these three mixtures up to total protein concentrations of 100 g/L. The agreement between model prediction and data is improved even further by allowing the designated mole fraction of proteins in each mixture to vary by a few percent from the nominal value, which is probably within the uncertainty to which molecular weights, and hence molar concentrations, can be determined experimentally by means of static light scattering.

Self-associating protein (chymotrypsin A)

The concentration dependence of the static light scattering of solutions of chymotrypsin A was measured at three pH values, and the data were plotted as a function of w/v concentration in Fig. 4 A–C. Since prior studies of the equilibrium self-association of chymotrypsin A performed at low protein concentrations (13–15) have established that the protein could form an equilibrium dimer, the data obtained in this study was modeled by expressions for the concentration dependence of light scattering by a mixture of monomer, equilibrium dimer, and possibly a third larger species in equilibrium with the monomer in a nonideal solution. Each of the species is represented within the model by an effective hard spherical particle having a mass corresponding to the stoichiometry of the assumed oligomer and a single specific volume common to all species. It was quickly established that a two-species (monomer-dimer) model could not account for the observed concentration dependence of scat-

tering over the entire range of concentrations to within experimental precision. Models incorporating monomer, equilibrium dimer, and one equilibrium higher-order oligomer of varying stoichiometry were then tried. It was found that to fit the experimental data to within experimental precision over the entire range of concentrations, it was necessary to postulate at least three significant species: monomer, dimer and, depending upon pH, either pentamer (pH 4.1 and 5.4) or hexamer (pH 5.4 and 7.2). The dependence of scattering upon concentration calculated at each pH according to the best-fit model or models with the best-fit parameter values presented in Table 2 is plotted together with the data in Fig. 4 A–C. In addition, the concentration dependent scattering calculated at each pH value for pure hard spherical monomer, dimer, pentamer and hexamer using the appropriate molar mass and the best-fit value of v_{eff} are plotted in the respective figures for comparison with the concentration dependence calculated according to the best-fit equilibrium scheme.

DISCUSSION

The effect of thermodynamic nonideality upon the light scattering intensity of interacting protein mixtures has previously been considered by Bajaj et al (29) and Alford et al (30). These prior treatments are subject to the following limitations. a), only first order deviations from thermodynamic ideality (two-body interactions or so-called second virial coefficient effects) are taken into account. b), only two

TABLE 2 Best-fit values of model parameters assuming various association schemes

pH	Self-association scheme	$\log K_2 \text{ (M}^{-1}\text{)}$	$\log K_n \text{ (M}^{-n+1}\text{)}$	$v_{\text{eff}} \text{ (cm}^3\text{/g)}$
7.2	Monomer-dimer- hexamer ($n = 6$)	3.45 (−0.15, +0.15)	16.67 (−0.29, +0.33)	0.86 (−0.10, +0.10)
5.4	Monomer-dimer- hexamer ($n = 6$)	3.76 (−0.17, +0.18)	16.49 (−0.37, +0.44)	1.58 (−0.20, +0.18)
	or	3.44 (−0.15, +0.14)	12.36 (−0.36, +0.24)	1.00 (−0.36, +0.20)
	Monomer-dimer-pentamer ($n = 5$)			
4.1	Monomer-dimer- pentamer ($n = 5$)	4.47 (−0.15, +0.17)	14.94 (−0.31, +0.34)	1.50 (−0.18, +0.14)

M_1 was fixed at a value of 23000 on the basis of results obtained from experiments carried out at low total concentration. Indicated uncertainties correspond to 1 standard error of estimate.

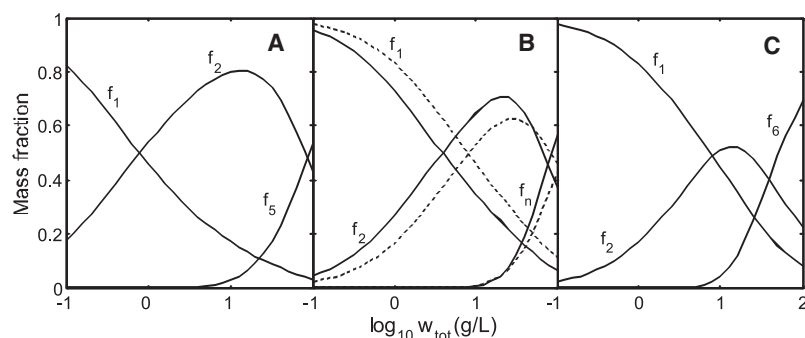


FIGURE 5 Fractional abundance of species plotted as a function of the logarithm of total protein concentration at pH 4.1 (A), 5.4 (B), and 7.2 (C), calculated as described in Minton et al (5) using the best-fit parameter values given in Table 2. Species abundance at pH 5.4 is calculated according to the best-fit monomer-dimer-hexamer model (solid curves) and the best-fit monomer-dimer-pentamer model (dashed curves).

scattering species (monomer and equilibrium dimer) are treated. The formalism of the treatments is such that extension to more complex interacting systems and more highly nonideal solutions (higher total protein concentration) would be prohibitively difficult. In contrast, the thermodynamic model used to interpret the data presented here (5) may be applied in a straightforward and parsimonious fashion to mixtures of an arbitrary number of interacting scattering species at arbitrarily high concentration.

The finding that the effective hard spherical particle model can fairly accurately predict the concentration dependence of light scattering of mixtures of noninteracting proteins at high total protein concentration reinforces the recent observation that the effective hard particle model provides a quantitative description of the concentration dependence of the osmotic pressure of an equimolar mixture of bovine serum albumin and ovalbumin over a range of concentration up to several hundred g/L (7). This finding also provides support for the validity of the greatly simplifying approximation, introduced above, that in solutions of moderate ionic strength, the effect of salt-protein interactions upon scattering may be treated implicitly as modulating protein-protein interaction instead of through attempting to explicitly evaluate the contribution of salt-protein cofluctuations to the summation indicated in Eq. 3.

The mass fraction of each significant association state of chymotrypsin, calculated using the best-fit model(s) with the best-fit parameter values presented in Table 2, is plotted as a function of the logarithm of total protein concentration at each pH value in Fig. 5 A–C. Inspection of these figures reveals that an equilibrium monomer-dimer model should suffice to account for the concentration dependence of scattering at total protein concentrations below ~ 10 g/L, but would be increasingly inadequate at higher concentrations where the equilibrium mass fraction of pentamer and/or hexamer becomes significant. It is noteworthy that the best-fit values of the monomer-dimer equilibrium association constant obtained from analysis of the present data at the two lower pH values are in good agreement with prior estimates of the pH dependence of the monomer-dimer equilibrium constant obtained from studies of chymotrypsin A at low concentration by sedimentation equilibrium (13,14) and static light scattering (15), as shown in Fig. 6.

The finding that an equilibrium between monomer and at least one oligomeric species larger than dimer must be invoked to account for the concentration dependence of light scattering of chymotrypsin A at high concentration is not surprising in view of earlier findings that other proteins not generally recognized as self-associating proteins, such as aldolase (28), ribonuclease A (31) and immunoglobulin G (32), may self-associate weakly at sufficiently high concentrations. The existence of a monomer- n -mer equilibrium with $n = 6 \pm 1$ in low concentration, low ionic strength solutions of chymotrypsin A at $\text{pH} > 8$ has been deduced from the concentration dependence of the weight-average sedimentation velocity (33) and the shape of trailing zonal boundaries in analytical gel filtration (34). The study presented here indicates that a significant mass fraction of a similar if not identical oligomeric species may exist in equilibrium with monomer and dimer even in solutions of substantially greater ionic strength and lower pH provided that the total protein concentration is sufficiently great.

According to the effective hard particle model, the extent to which the effective specific volume of a protein species exceeds the partial specific volume is a measure of the

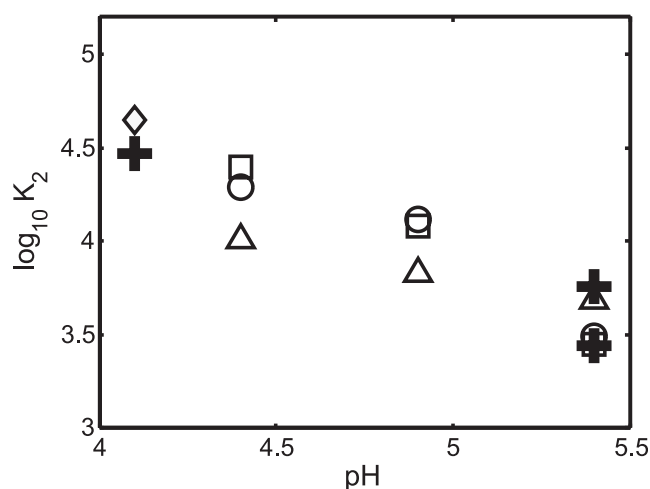


FIGURE 6 Comparison of values of the pH-dependent monomer-dimer equilibrium constant presented in Table 2 (+ symbols) with values previously reported for chymotrypsin A in the literature (all other symbols as indicated in the caption to Fig. 4 B of reference 15).

magnitude of soft repulsive interactions between like molecules, and generally increases with the net charge of the macromolecule under a given set of conditions (11,8). According to the present analysis, the effective specific volume of chymotrypsin A increases with decreasing pH. This is attributed to increasing net positive charge as solution pH decreases below 8.8, the isoelectric point of the protein (35).

The success of the effective hard particle model in accounting for the concentration dependent light scattering of mixtures of BSA, ovalbumin, and ovomucoid indicates that repulsive interactions between like and unlike protein molecules in these solutions are approximately additive. Note that this finding is not equivalent to the statement that the model for scattering is additive in the scattering of individual species, which is shown by the data presented in Fig. 1–3 to be clearly untrue at high total concentration.

In the language of this model, the distance between the centers of effective spheres representing species i and j at close contact, denoted by r_{ij} , may be approximated by

$$r_{ij} \approx (r_{ii} + r_{jj})/2. \quad (4)$$

The validity of this approximation is attributed to the fact that all three proteins have isoelectric points between 4.4 and 4.8 (35,36), and thus bear net negative charges at the pH of measurement. At present it is unclear whether the effective hard particle model can be generalized to treat the case of mixtures of concentrated proteins bearing unlike charges (24). It will be important to study such systems, both theoretically and experimentally, since one would expect complex biological fluid media to contain a variety of proteins and other macromolecules bearing both positive and negative net charge at the ambient pH in vivo.

The authors thank Peter McPhie, National Institute of Diabetes and Kidney Diseases, for helpful comments on a draft of this report.

This research was supported by the Intramural Research Program of the National Institute of Diabetes and Digestive and Kidney Diseases, National Institutes of Health.

REFERENCES

1. Zhou, H. -X., G. Rivas, and A. P. Minton. 2008. Macromolecular crowding and confinement: biochemical, biophysical and potential physiological consequences. *Ann. Rev. Biophys.* 37:375–397.
2. Zimmerman, S. B., and A. P. Minton. 1993. Macromolecular crowding: biochemical, biophysical, and physiological consequences. *Annu. Rev. Biophys. Biomol. Struct.* 22:27–65.
3. Shire, S. J., Z. Shahrokhi, and J. Liu. 2004. Challenges in the development of high protein concentration formulations. *J. Pharm. Sci.* 93:1390–1402.
4. Ross, P. D., and A. P. Minton. 1977. Analysis of nonideal behavior in concentrated hemoglobin solutions. *J. Mol. Biol.* 112:437–452.
5. Minton, A. P. 2007. Static light scattering from concentrated protein solutions I. General theory for protein mixtures and application to self-associating proteins. *Biophys. J.* 93:1321–1328.
6. Minton, A. P. 2007. The effective hard particle model provides a simple, robust, and broadly applicable description of nonideal behavior in concentrated solutions of bovine serum albumin and other nonassociating proteins. *J. Pharm. Sci.* 96:3466–3469.
7. Minton, A. P. 2008. Effective hard particle model for the osmotic pressure of highly concentrated binary protein solutions. *Biophys. J.* 94:L57–L59.
8. Minton, A. P., and H. Edelhoch. 1982. Light scattering of bovine serum albumin solutions: extension of the hard particle model to allow for electrostatic repulsion. *Biopolymers.* 21:451–458.
9. Rivas, G., J. A. Fernandez, and A. P. Minton. 1999. Direct observation of the self-association of dilute proteins in the presence of inert macromolecules at high concentration via tracer sedimentation equilibrium: theory, experiment, and biological significance. *Biochemistry.* 38:9379–9388.
10. Ross, P. D., R. W. Briehl, and A. P. Minton. 1978. Temperature dependence of nonideality in concentrated solutions of hemoglobin. *Biopolymers.* 17:2285–2288.
11. Minton, A. P. 1995. A molecular model for the dependence of the osmotic pressure of bovine serum albumin upon concentration and pH. *Biophys. Chem.* 57:65–70.
12. Fernández, C., and A. P. Minton. 2008. Automated measurement of the static light scattering of macromolecular solutions over a broad range of concentrations. *Anal. Biochem.* 381:254–257.
13. Morimoto, K., and G. Kegeles. 1967. Dimerization and activity of chymotrypsin at pH 4. *Biochemistry.* 6:3007–3010.
14. Aune, K., and S. N. Timasheff. 1971. Dimerization of alpha-chymotrypsin I. pH dependence in the acid region. *Biochemistry.* 10:1609–1617.
15. Kameyama, K., and A. P. Minton. 2006. Rapid quantitative characterization of protein interactions by composition gradient static light scattering. *Biophys. J.* 90:2164–2169.
16. Kirschenbaum, D. M. 1976. Molar absorptivity and $A_{1\text{ cm}}^{1\%}$ values for proteins at selected wavelengths in the ultraviolet and visible region. In *Handbook of Biochemistry and Molecular Biology*. G. D. Fasman, editor. CRC Press, Cleveland, pp. 383–545.
17. Davis, J. G., C. J. Mapes, and J. W. Donovan. 1971. Batch purification of ovomucoid and characterization of the purified product. *Biochemistry.* 10:39–42.
18. Attri, A. K., and A. P. Minton. 2005. New methods for measuring macromolecular interactions in solution via static light scattering: basic methodology and application to nonassociating and self-associating proteins. *Anal. Biochem.* 337:103–110.
19. Theisen, A., C. Johann, M. P. Deacon, and S. E. Harding. 2000. *Refractive Increment Data-book*. Nottingham University Press, Nottingham. 55.
20. Stacey, K. A. 1956. *Light-scattering in physical chemistry*. Academic Press, New York.
21. Stockmayer, W. H. 1950. Light scattering in multi-component systems. *J. Chem. Phys.* 18:58–61.
22. Asthagiri, D., A. Paliwal, D. Abras, A. M. Lenhoff, and M. E. Paulitis. 2005. A consistent experimental and modeling approach to light-scattering studies of protein-protein interactions in solution. *Biophys. J.* 88:3300–3309.
23. Winzor, D. J., M. Deszczynski, S. E. Harding, and P. R. Wills. 2007. Nonequivalence of second virial coefficients from sedimentation equilibrium and static light scattering studies of protein solutions. *Biophys. Chem.* 128:46–55.
24. Hall, D., and A. P. Minton. 2003. Macromolecular crowding: qualitative and semiquantitative successes, quantitative challenges. *Biochem. Biophys. Res. Commun.* 1649:127–139.
25. Boublik, T. 1974. Statistical thermodynamics of convex molecule fluids. *Mol. Phys.* 27:1415–1427.
26. Lebowitz, J. L., E. Helfand, and E. Praestgaard. 1965. Scaled particle theory of fluid mixtures. *J. Chem. Phys.* 43:774–779.
27. Hill, T. L., and Y. -D. Chen. 1973. Theory of aggregation in solution I. General equations and application to the stacking of bases, nucleosides, etc. *Biopolymers.* 12:1285–1312.

28. Muramatsu, N., and A. P. Minton. 1989. Hidden self-association of proteins. *J. Mol. Recognit.* 1:166–171.
29. Bajaj, H., V. K. Sharma, and D. S. Kalonia. 2007. A high-throughput method for detection of protein self-association and second virial coefficient using size-exclusion chromatography through simultaneous measurement of concentration and scattered light intensity. *Pharm. Res.* 24:2071–2083.
30. Alford, J. R., S. C. Kwok, J. N. Roberts, D. S. Wuttke, B. S. Kendrick, et al. 2008. High concentration formulations of recombinant human interleukin-1 receptor antagonist: I. Physical characterization. *J. Pharm. Sci.* 97:3035–3050.
31. Zorrilla, S., M. Jiménez, P. Lillo, G. Rivas, and A. P. Minton. 2004. Sedimentation equilibrium in a solution containing an arbitrary number of solute species at arbitrary concentrations: theory and application to concentrated solutions of ribonuclease. *Biophys. Chem.* 108:89–100.
32. Jiménez, M., G. Rivas, and A. P. Minton. 2007. Quantitative characterization of weak self-association in concentrated solutions of Immunoglobulin G via the measurement of sedimentation equilibrium and osmotic pressure. *Biochemistry.* 46:8373–8378.
33. Pandit, M. W., and M. S. Narasinga Rao. 1974. Studies on self-association of proteins. The self-association of alpha-chymotrypsin at pH 8.3 and ionic strength 0.05. *Biochemistry.* 13:1048–1055.
34. Ackers, G. K., and T. E. Thompson. 1965. Determination of stoichiometry and equilibrium constants for reversibly associating systems by molecular sieve chromatography. *Proc. Natl. Acad. Sci. USA.* 53:342–349.
35. Malamud, D., and J. W. Drysdale. 1978. Isoelectric points of proteins: a table. *Anal. Biochem.* 86:620–647.
36. Rhodes, M. B., P. R. Azari, and R. E. Feeney. 1958. Analysis, fractionation and purification of egg white proteins with cellulose-cation exchanger. *J. Biol. Chem.* 230:399–408.